

A Large Slipping Finite Element Model for Geosynthetics Interface Modeling

Yi, Chang – Tok*

요 지

보강토구조물은 흙과 보강재 사이에 큰 변형이 발생하며 보강토구조물의 파괴양상도 보강재의 미끄러짐이나 변형에 의해 지배되며, 때때로 보강재의 재료의 파괴보다는 미끄러짐에 의해 보강토구조물이 파괴되므로 큰변형이 발생하는 흙-보강재의 모델링이 필요하다.

고형 및 액체폐기물 매립장에 쓰이는 라인너 시스템은 매립장의 경사와 쓰레기하중에 의해 큰 변형이 발생하게 된다. 이러한 큰 변형의 문제는 기존의 접촉요소로써 모델링하는데 많은 제약이 따른다.

본 논문에서는 이러한 흙과 토목섬유보강사이의 큰 변형을 모델링할 수 있는 접촉요소를 제안하였으며, 그 이론과 그 모델의 적용성에 대하여 논하였다.

Abstract

Reinforced soil structures may experience large local movements between soil and reinforcement. The failure modes of a reinforced structure depend on several factors which are governed by deformation and slipping of the reinforcement. In some cases, pulling out of the reinforcement may occur instead of rupturing. The growing use of geosynthetic liner system for storage of solid and liquid wastes has led to a number of slope instability problems where the synthetic liner may undergo a large amount of stretching and slipping as a result of the loading. The conventional finite element model for the soil-reinforcement interface uses a zero thickness joint element with normal and shear stiffnesses and can only accommodate a small amount of deformation. When a large slippage occurs, the model provides an incorrect mechanism for deformation.

This paper presents a new interface finite element model which is able to simulate a large amount of slippage between soil and reinforcement. The formulation of the model is presented and the capability of the model is demonstrated using illustrative examples.

Keywords : Shear Stiffness, Normal Stiffness, Large Slippage, Geosynthetics, Interface Model.

* Member, Project manager, Piletech

1. Introduction

Reinforced soil structures may experience large local movements between soil and reinforcement. Some failure modes of a reinforced structure depend on several factors which are governed by deformation and slipping of the reinforcement. In some cases, pulling out of the reinforcement may occur instead of rupturing. The growing use of geosynthetic liner systems for storage of solid and liquid wastes has led to a number of slope instability problems where the synthetic liner undergoes a large amount of stretching and slipping as a result of the loading. The conventional finite element model for the soil-reinforcement interface uses a zero thickness joint element with normal and shear stiffnesses and can only accommodate a small amount of deformation. When a large slippage occurs, this model provides an incorrect mechanism for deformation.

Several types of finite elements have been proposed for the modeling of joints and interfaces which can be classified into four categories (Gens et al., 1988). The interface element formulated on the basis of relative displacements between opposite nodes has been widely used in the finite element analysis of soil-structure interaction (Wu, 1992). These interface elements can be divided into two groups: finite thickness (Sharma et al., 1992; Desai et al., 1984) and zero thickness interface elements (Andrews et al., 1982; Gens et al., 1990).

The zero thickness interface element is based on the joint element proposed by Goodman et al. (1968). The formulation of the model is based on the relative displacements between surfaces of rock joints with two set of springs, one acting parallel to the interface (K_s) and the other acting perpendicular to it (K_n). The shear stiffness (K_s) representing the relationship between the shear stress and relative displacements of the solid elements surrounding the interface plays an important role in determining the interface behavior. The assumed value of the normal stiffness (K_n) representing the relationship between the normal stress and the relative displacement is normally high so that the interface does not overlap. However, it may not be appropriate to assign an arbitrarily high value for the normal stiffness. Because the interface is surrounded by the soil and geosynthetics, its normal stiffness properties during the deformation process must depend on the characteristics of the interface zone as well as the state of stress and properties of the surrounding elements. The joint element approach does not provide realistic modeling of the normal stress in soil-structure interaction, even though it provides satisfactory prediction of the shear behavior (Desai et al., 1984). It is difficult to arrive at an appropriately high value for K_n which yields reliable results.

A thin solid element to simulate the interface behavior was proposed by Desai et al. (1984) which provides satisfactory solutions for various deformation modes such as debonding when the normal stress becomes tensile. However, the element thickness cannot be determined easily for soil-structure interface problems. Too small a thickness causes computational difficulties and the thin layer element behaves like a solid element. The recommended solution for choosing an element thickness is based on a parametric study in

which the solutions for different thicknesses are compared with observation data. However, the parameters expressing the constitutive relationship of the interface element are exactly the same as the zero thickness interface element. The normal stiffness of this interface element is chosen based on the state of stress in the interface element which provides improved calculation of the interface normal stresses. However, arbitrary values of the normal stiffness are often chosen. This approach may not be realistic in soil-structure interaction problems, and can result in erratic and unrealistic normal stress at the interface (Sharma et al., 1992).

Herrmann (1978) presented an algorithm for interface element similar to the zero thickness interface concepts with certain improvements through constraint conditions. However, the normal stiffness and shear stiffness during sliding were still chosen arbitrarily.

In the case of reinforced soil structures, the failure mode of the reinforcement imbedded in the soil depends on the geometry of the reinforcement, soil type, imbedded length, normal stress, and especially the stiffness and tensile strength of the reinforcement. Costalonga(1988) carried out pull-out tests using a HDPE geogrid and a PET geogrid in a silty clay. It is interesting to note that the reinforcement failed owing to slippage between soil and reinforcement rather than rupturing of the reinforcement. For geosynthetic reinforcements such as geogrids or high strength woven reinforcement, the load-strain relationship generally remains quite linear during the pull-out test, indicating that these reinforcements are stiff enough to have slippage of the reinforcement in the reinforced soil structures. Therefore, it is important that, in modeling the interface of a reinforced soil, finite slippage must be simulated.

The growing use of geosynthetics liner systems for waste or liquid containment has led to a number of slope instability problems. As the waste material is dumped into the waste containment, the shear forces between soil and geosynthetics in a liner system increase rapidly. To maximize the volume of disposal, the stability of steep side slopes is of high economic interest. The frictional properties of the system have to be examined in order to find out if there are any potential sliding surfaces under high shear stresses. In such a case, a large amount of slipping or stretching of geosynthetics occurs along the interface between the geosynthetic and soil or between geosynthetic layers. A common failure mechanism of

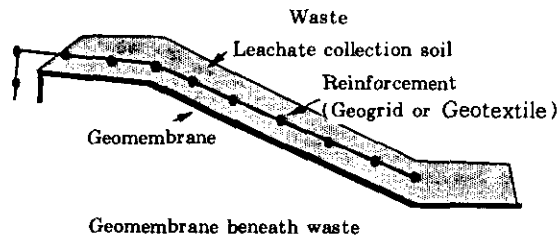


Fig 1. Solid Waste Containment System with Reinforcement

geomembrane lined slopes is by slippage of components within the liner system or of the owing to excessive shear stresses.

Whenever a geomembrane-lined slope is covered with soil, a stability for the slope should be calculated to assess the potential for sliding failure of the soil or tension failure of the geomembrane. A stability failure of the slope should be sliding of cover soil on the geomembrane. To increase the stability of the slope, geogrid or geotextile reinforcement is added in the liner systems as shown in Fig 1. The stresses in the reinforcement are generally carried to an anchor which extends behind the geomembrane anchor trench. As the landfill is filled, the shear forces are mobilized rapidly, which trigger the sliding failure of the slope. Since the normal forces on the reinforcement or geomembrane may be smaller than the shear forces, the frictional resistance along the reinforcement is small, allowing displacement to occur over the entire length of the reinforcement. In this case, slippage or a large amount of relative displacement between the soil and reinforcement may occur.

In this paper, a new interface finite element model is proposed. The constitutive law for the thin thickness interface or the zero thickness interface element is defined by expressing the constitutive matrix in terms of the normal and shear characteristics. However, in the large slippage interface model the constitutive behavior is incorporated during the solution process of the finite element scheme, and complete compatibility between the soil and the reinforcement is always satisfied without a high value of the normal stiffness which may result in erratic normal stresses at the interface. This model adopts a contact approach in which the soil and reinforcement are treated as surfaces of contact between two bodies (Bathe et al., 1985). The model can simulate a large amount of slipping between the soil and the reinforcement. Compatibility is satisfied by using the Lagrange multipliers constraint approach to ensure no overlapping of materials. Separation of the soil and reinforcement can be modeled easily by using this approach. Normal and frictional forces develop at the interface according to the stiffnesses of the materials. The interfacial strength between the soil and the reinforcement is assumed to be governed by the Coulomb frictional law which accounts for both frictional and passive resistance of the geogrid reinforcement.

2. Model Formulation

2.1 Imposition of Constraints

A specific constraint can be applied on the interface between the soil and reinforcement boundary. The normal displacements along the reinforcement should be the same as those of the soil to prevent overlapping of the materials. These conditions specify the normal displacements along the soil and the reinforcement and must satisfy the compatibility condition. Therefore, there is no need to adopt a high value of normal stiffness as is done in the thin interface model. Separation of the soil and reinforcement can be modeled easily by providing specified normal displacements at the soil-reinforcement interface.

The Lagrange multiplier method is used to incorporate constraints in the variational or

weighted residual methods. The Lagrange multiplier method has been used in many fields of mathematics and physics to impose constraint conditions on algebraic or differential equations (Matthew and Walker, 1964). Considering the variational formulation of a discrete system, the functional Π can be expressed as follows (Bathe, 1982):

$$\Pi = \frac{1}{2} U^T K U - U^T R \quad (1)$$

where U is a vector of global displacement ;

K is the element stiffness matrix ;

R is a vector of forces acting in the direction of global displacement.

The variation with respect to displacements, U_i could be written as

$$\frac{\partial \Pi}{\partial U_i} = 0 \quad (\text{for all components of } i)$$

Equation (2) indicates that the functional Π , the total potential energy in this case, is not only stationary but is a minimum value for an approximate finite element solution. The boundary condition for Equation (1) can be considered as a constraint on the variational formulation. If we impose a constraint U_i^* on the displacement U_i such that $U_i = U_i^*$ then we can rewrite the constraint variational Π^* as

$$\Pi^* = \frac{1}{2} U^T K U - U^T R - \lambda (U_i - U_i^*) \quad (3)$$

where λ is a Lagrange multiplier.

Invoking the stationary condition, we obtain

$$\delta U^T K U - \delta U^T R + \lambda \delta U_i + \delta \lambda (U_i - U_i^*) \quad (4)$$

variations δU and $\delta \lambda$ are arbitrary values and the above equation yields the following matrix form :

$$\begin{bmatrix} K & K_c^T \\ K_c & 0 \end{bmatrix} \begin{Bmatrix} U \\ \lambda \end{Bmatrix} = \begin{Bmatrix} R \\ 0 \end{Bmatrix} \quad (5)$$

where K_c is a rectangular matrix which contains the constraint conditions $U_i - U_i^*$. The size of the K_c matrix is related to the number of constraint conditions, and each row of matrix possesses two non-zero values, 1 and -1 corresponding to the constrained displacement columns in the matrix; K is the stiffness matrix which can be easily calculated in the conventional finite element procedures.

The coefficient matrix in the above Equation (5) is symmetric if K is symmetric. However, the diagonal elements in the coefficient matrix corresponding to the Lagrange multiplier are zero. This causes computational difficulties unless the solution process allows for zero diagonal terms. The constraint method can be used to impose connection between any two nodes in the finite element domain. To maintain compatibility between the soil and the reinforcement the normal displacements of the corresponding nodes are connected un-

less tension occurs at the interface. This scheme avoids the use of the high normal stiffness found in a traditional interface model.

2.2 Horizontal Constraints

The stress transfer mechanism between soil and grid reinforcements involves frictional and passive soil resistance at the soil-reinforcement interface. In the reinforced soil structure the primary mechanism of stress transfer is through frictional resistance. However, passive resistance plays an important role when grid reinforcements are employed.

The large slipping interface model has adapted the shear stiffness (K_s) in applying a horizontal resistance along the reinforcement. The shear stiffness (K_s) appears as the initial slope of the shear stress-displacement curve measured in the pull-out test or the shear box test. However, pull-out tests are known to provide a better simulation of the interface behaviour between the soil and the reinforcement (Garbulewski, 1990). Pull-out resistance includes passive and frictional resistance, i.e., the shear stiffness obtained consists of stiffness from both frictional and passive resistance components. The total equivalent initial shear stiffness (K_s) is the sum of these two components. Thus, a proper choice of shear stiffness (K_s) can simulate the horizontal resistance of geogrid reinforcement (Chan et al., 1993). Pull-out tests provide the relationship between the shearing resistance and the displacement at the pull-out slot; therefore, it is necessary to calculate the shear stress in order to obtain the shear stiffness.

In a small displacement problem, the shear stiffness is assumed to be linear and is equal to the initial slope of the shear stress-displacement curve. A hyperbolic formula can be used for the shear stress-displacement relationship. However, the variation of peak and residual shear strengths with the relative displacement should be used for a large slippage model. An idealization constitutive law for the shear stress-displacement behaviour is shown in Fig. 2. The limiting shear stress τ_p is assumed to be governed by the Coulomb frictional law. If the shear stress exceeds τ_p , the shear stress falls to a residual value τ_r , and the mobilized shear stress on the reinforcement becomes constant.

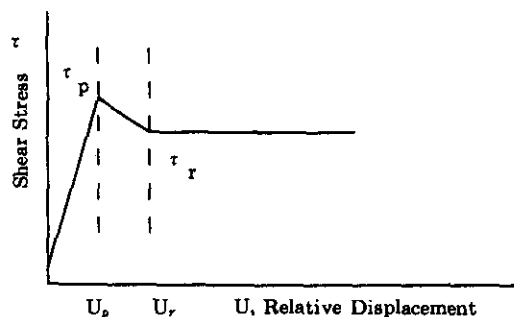


Fig. 2. Constitutive Law for Shear-Displacement Behaviour

The procedure for implementing the frictional resistance on the reinforcement is explained in Fig 3. First node displacements are calculated by imposing the displacement constraints at the interface using the Lagrange multiplier. Relative displacements are calculated between the soil and the reinforcement and the shear stresses developed are determined. The failure criterion is checked for possible slippage at the interface. Additional nodal forces are imposed owing to the changes in stresses at the interface and further displacements are calculated until the system has reached an equilibrium state.

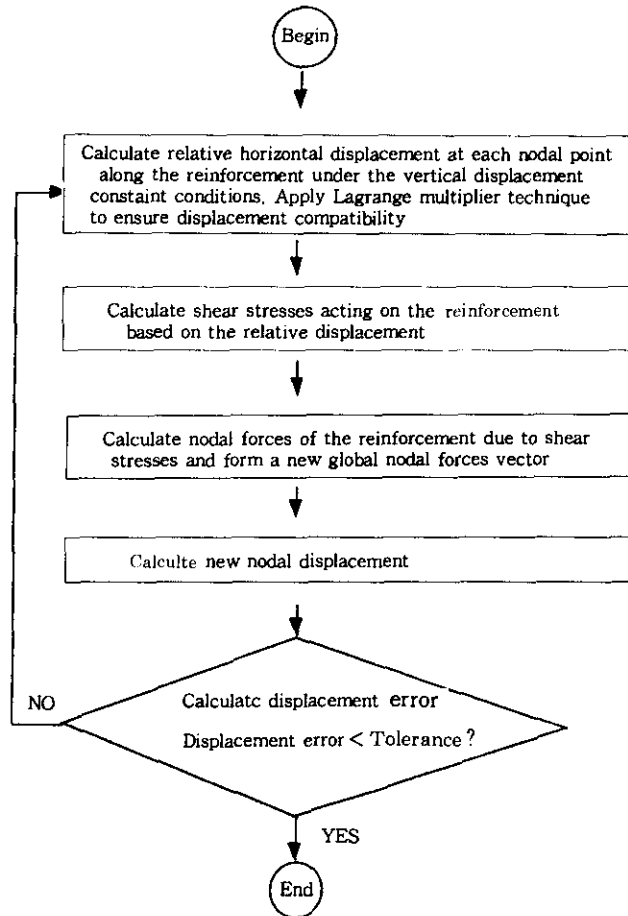


Fig 3. Flow Chart for Application of Horizontal Resistance on Reinforcement

3. Solution Strategy

The finite element method requires the solution of simultaneous algebraic equations. Each diagonal coefficient of the stiffness matrix is always positive definite, and the stiffness matrix is banded and symmetric. However, there are still many zero elements within the bandwidth. The skyline method(Felippa, 1975) utilizes the concept of variable

bandwidth in which only non-zero elements under skyline are stored and used in the calculation. Many solution schemes have been proposed by using the above properties of the stiffness matrix.

However, each diagonal coefficient of the stiffness matrix with the imposed constraint condition is no longer positive definite and many diagonal coefficients of stiffness matrix are zero. The solution to Equation(5) can be obtained by using the Gauss-Elimination method.

The overall Gauss elimination procedure applied to the $n \times (n+1)$ augmented matrix is condensed into a three-part mathematical formula for initialization, elimination, and back substitution. Elimination formula can be expressed as follows:

$$\{R\} = [K] \{U\} \quad (6)$$

Where $\{R\}$ is a vector of global displacements :

$[K]$ is the element stiffness matrix

$\{U\}$ is a vector of forces acting in the direction of global displacements

$$K_{i,j}^{(k)} = K_{i,j}^{(k-1)} - \frac{K_{k,k}^{(k-1)}}{K_{k,k}^{(k-1)}} K_{k,i}^{(k-1)} \quad (7)$$

where $j = n+1, n, \dots, k : k = 1, 2, \dots, n-1$

$i = k+1, k+2, \dots, n$

The counter k is the iteration counter of the outside loop in a set of nested loops that perform the elimination. It should be noted that the element K_{ii} in the denominator of Equation (7) is always the diagonal element. It is called the pivot element. The pivot element must not be zero; otherwise, the computer program will result in overflow. The computer program can be written so that it rearranges the equations at each step to attain diagonal dominance in the coefficient matrix, i.e., the row with the largest pivot element is chosen. This strategy is called partial pivoting, and it serves two purposes in the Gaussian elimination procedure: it reduces the possibility of division by zero and it increases the accuracy of the Gauss elimination method using the largest pivot element. If the column is also searched for the maximum available pivot element, then the strategy is called complete pivoting. If pivoting cannot locate a non-zero element to place on the diagonal, the matrix is singular. When two columns are interchanged, the corresponding variable must also be interchanged. A program which performs complete pivoting must keep track of the column interchanges in order to interchange the corresponding variables.

4. Application

To illustrate the effectiveness of the model, a simple reinforced soil sample under plane strain condition is shown in Fig. 4. A surface traction of 2.0 kPa was applied at the top of the soil element in the first loading step of the simulation. Then a prescribed 1m horizontal displacement was imposed on the free end of the reinforcement to simulate the pull-out

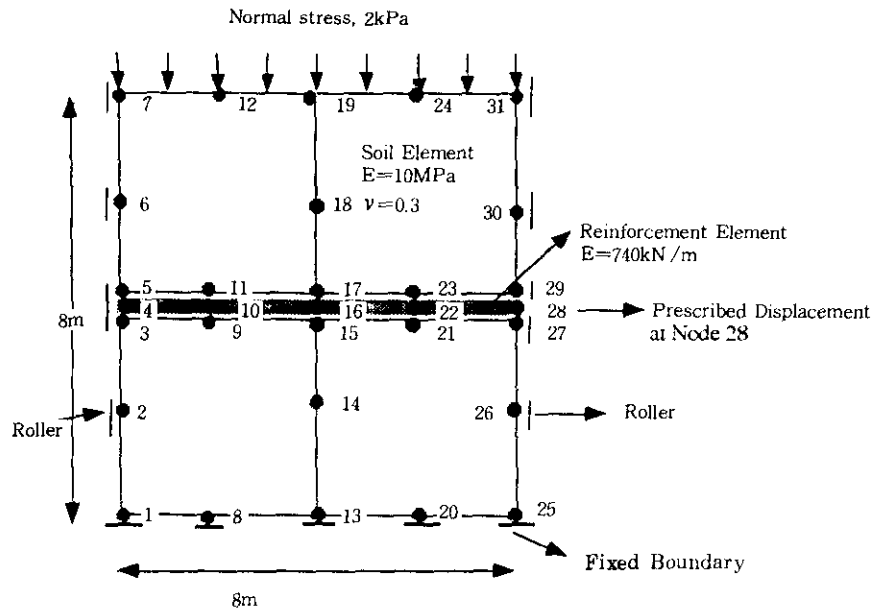


Fig 4. Reinforced Soil Structure

test. The prescribed displacement was applied in two loading steps to ensure that a large displacement or slipping of the reinforcement can be simulated properly in the large slipping interface model. The material properties are shown in Fig 4.

The vertical displacements of nodes 3, 4 and 5 should be the same to prevent overlapping of the materials. The same condition applies on all other nodes along the reinforcement. A total of 10 constraints was imposed on the stiffness matrix as displacement constraint conditions. The shear stiffness K_s was assigned 10 kN/m^3 for the horizontal constraints.

When slipping occurred, the mobilized shear stress remained relatively constant over a portion of the reinforcement. However, the mobilized shear stress on the reinforcement was assumed to increase linearly with the relative displacement between the soil and the re-

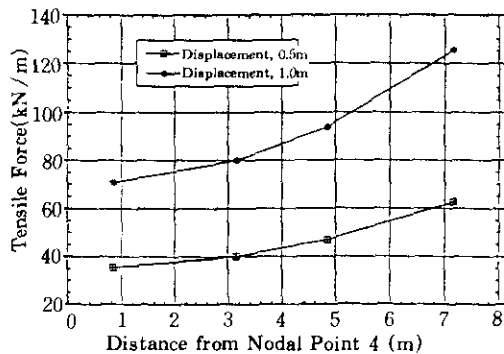


Fig 5. Tensile Force Distribution along the Reinforcement

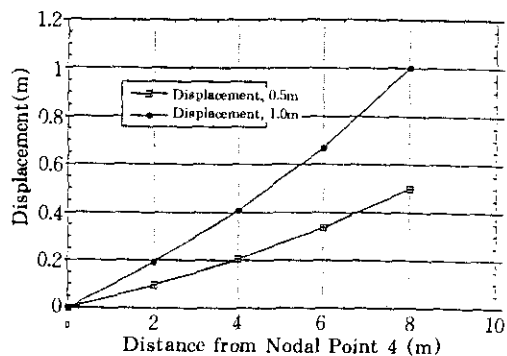


Fig 6. Displacement Distribution along the Reinforcement

inforcement to ensure that the horizontal constraint works properly. Without any horizontal constraint, it was found that the mobilized shear stress along the reinforcement was zero.

Fig 5. shows the tensile stress along the reinforcement at 1m displacement under both constraint conditions. The vertical displacement constraints and compatibility conditions between the soil and the reinforcement were always satisfied at any loading step as shown in Table 1. Fig 6. shows the distribution of nodal horizontal displacements along the reinforcement.

Table 1. Vertical Displacement at 1m Horizontal Displacement

Node	3, 4 & 5	9, 10 & 11	15, 16 & 17	21, 22 & 23	27, 28 & 29
Displacement(m)	-0.03593	-0.03617	-0.03585	-0.0362	-0.03577

The simulation of the slippage of reinforcement is a main concern in this interface element. When the horizontal displacement of the reinforcement was increased, node 4 was between node 5 and node 11 after several steps (Fig 4.). In this case, the constraint conditions for compatibility between the soil and reinforcement should be considered to simulate the slippage of reinforcement. The element interpolation functions can be used to calculate the normal displacement of the reinforcement at any point between two nodal points which correspond to the soil nodal points. However, an approximate method was used in this case. After calculating the horizontal relative displacement between the soil

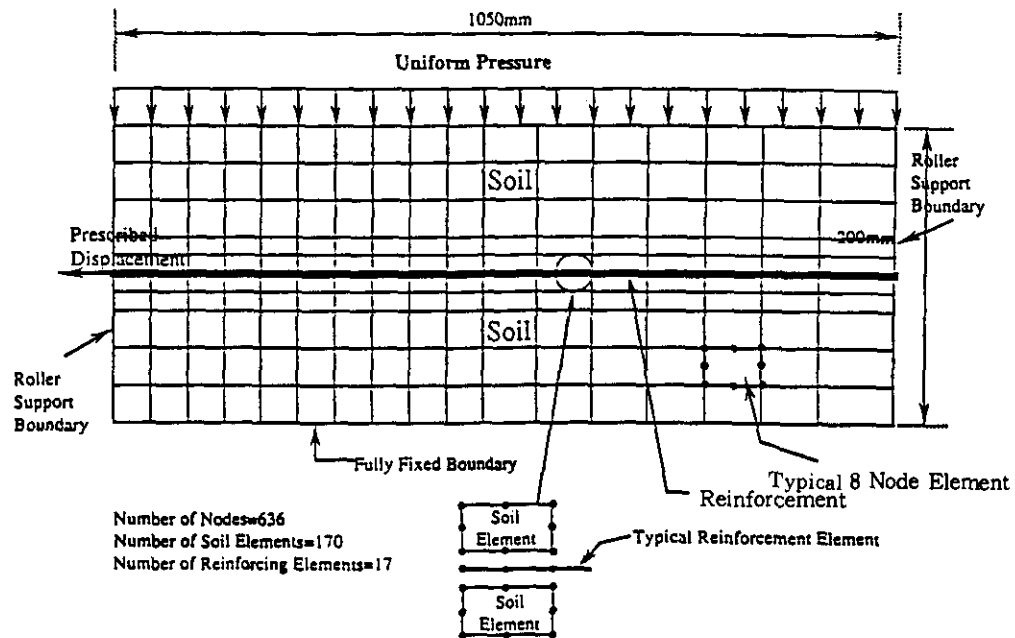


Fig 7. Finite Element Idealization of Soil and Reinforcement for the Pull-out Test

and the reinforcement, the reinforcement node was associated with the nearest soil node. For instance, if node 4 was located between node 5 and node 11, the constraint conditions would be applied based on nodes 5 or 11 depending on the proximity of the nodes to satisfy compatibility conditions. A stretching strain mode of the reinforcement, i.e, the horizontal displacement of the reinforcement in Fig. 4, would be expected. Therefore, this approximate method will not cause any calculation error.

To illustrate the capacity of the model for practical applications, the pull-out test conducted by Costalonga (1988) was analyzed. A two dimensional plane strain finite element mesh is shown in Fig 7. The material properties can be found in Chan et al.(1993)

A shear stiffness of 540 kN/m^3 calculated from the conventional method without any correction was used for the horizontal constraint. The calculated force-displacement response is compared with the pull-out test as shown in Fig 8. It is seen that a maximum pull-out resistance was reached at a displacement of 3.7cm when the full length of the reinforcement was displacing at the same rate. Fig 9. shows that the mobilized tensile stresses on the reinforcement at a displacement of 3.7cm increased linearly along the entire length of the reinforcement, i.e., the mobilized shear stresses were constant, indicating that

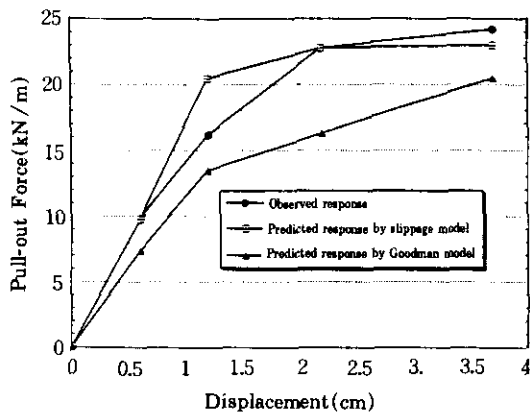


Fig 8. Force-Displacement Response of the Reinforcement in the Pull-out Test

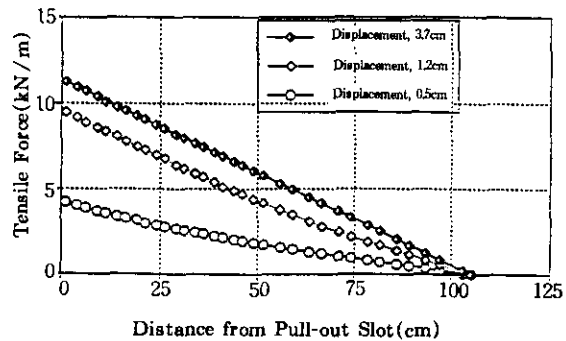


Fig 9. Tensile Force Distribution along the Reinforcement

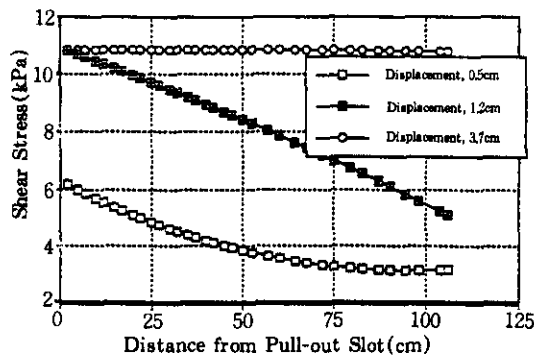


Fig 10. Shear Stress Distribution along the Reinforcement

the total length of the reinforcement was slipping. It was illustrated that the slippage of the reinforcement developed at the front part of the reinforcement at a displacement of 1.2cm. The distribution of shear stress along the reinforcement at a displacement of 1.2cm is not uniform since the tensile force in the reinforcement decreases away from the point of application of the pull-out forces. As the reinforcement is further pulled through the soil, a maximum shear stress is reached along the entire length of the reinforcement as shown in Fig 9. This progressive shearing is shown in Fig 9.

5. Conclusion

A new large slipping finite element model for geosynthetic interface models has been introduced. When using the constraint approach such as the Lagrange multiplier method it is not necessary to choose arbitrarily high values for the normal stiffness (K_n) to satisfy compatibility between the soil and the reinforcement. The shear stiffness (K_s) is used to apply horizontal resistance along the reinforcement which can account for both frictional and passive soil resistance of geogrid reinforcement. A simple reinforced soil structure example and an analysis of a pull-out test were used to demonstrate that this model can easily simulate a large amount of slipping between the soil and the reinforcement. The results of the analysis of the pull-out test with the proposed method showed good agreement with the measured behavior. Although no attempt is made to do so in this paper, clearly, the approach can be any soil-structure interaction problem which involves a large amount of slipping. However, the presence of the constraints leads to increases in bandwidth of the equations to be solved and also produced zero diagonal terms in the stiffness matrix. These numerical difficulties require the computation time to increase, and a new solution scheme need to be developed as a further study.

Notations

$[K]$	Stiffness matrix
K_c	Rectangular matrix containing constraint conditions
K_n	Normal stiffness
K_s	Shear stiffness
λ	Lagrange multiplier
Π	Functional
$\{R\}$	Vector of forces
τ_r	Residual shear stress
τ_p	Peak shear stress
$\{U\}$	Vector of global displacement

References

1. Andrews, K.Z., McGown, A., Wilson-Fahmy, R.F. and Mashhour, M.M.(1982), "The Finite Element Method of Analysis Applied to Soil-geotextile", *Proc. 2nd Int. Conf. on Geotextiles*, Vol.3, pp.695-700.
2. Bathe, K.J.(1982), *Finite Element Procedures in Engineering Analysis*, Prentice-Hall, Inc. New York.
3. Bathe, K.J. and Chaudhary, A.(1985), "A Solution Method for Planar and Axisymmetric Contact Problems", *Journal for Numerical Methods in Engineering*, Vol. 21, pp. 65-88.
4. Chan, D.H. Yi, C.T. and Scott, J.D. (1993). "An Interpretation of the Pull-Out Test", *Proc. Geosynthetics '93 Conference*, Vancouver, Canada, Vol.2, pp.593-605.
5. Costalonga, M.A.R. (1988), Geogrid Pull-out test in Clay, M.Sc. Thesis, The University of Alberta, Edmonton, Alberta, Canada.
6. Desai, C.S., and Zaman, M.M., (1984), "Thin-layer Element for Interfaces and Joints", *International Journal for Numerical and Analytical Methods in Geomechanics*, Vol.8, pp.19-43.
7. Garbalewski, K. (1990), "Direct Shear and Pull-out Resistance at the Geotextile Interface", *Proceeding of the Fourth International Conference on Geotextiles Geomembrane and Related Product*, Hague, Netherlands, pp. 737-742.
8. Gens, A., Caro, I. and Alonso, E.E.(1988), "An Interface Element Formulation for The Analysis of Soil Reinforcement Interaction", *Com. and Geotech.*, Vol.7, pp.133-151.
9. Goodman, R.E., Taylor, R.L. and Brekke, T.L. (1968), "A Model for the Mechanics of Jointed Rock", *Journal of Soil Mechanics and Foundation Engineering Division*, ASCE, Vol.94, No.SM 3, pp. 637-659.
10. Herrmann, L.R.(1978), "Finite Element Analysis of Contact Problems", *J.Eng.Mech.*, ASCE, Vol. 104, pp.1043-1059.
11. Matthew, J. and Walker, R.L.(1964), *Mathematical Methods of Physics*, Benjamin New York.
12. Sharma, K.G., and Desai, C.S.(1992), "Analysis and Implementation of Thin-layer Element for Interface and Joints", *J.Eng.Mech.*, ASCE, Vol.118, No.12, pp.2442-2462.
13. Wu, J.T.H.(1992), "Discussions: Embankment", *Pro. Int. Sympo.on Earth Reinforcement Practice*, Kyushu, Japan, Vol.2, pp.928-929.

(received on Jan. 5, 1996)